Biogeosciences Discuss., 12, 11797–11831, 2015
www.biogeosciences-discuss.net/12/11797/2015/
doi:10.5194/bgd-12-11797-2015

Biogeosciences Discussions
Open Access

Nonlinear thermal and moisture dynamics of high Arctic wetland polygons following permafrost disturbance

E. Godin[1,3], **D. Fortier**[1,3], **and E. Lévesque**[2,3]

[1]Université de Montréal, Montréal, Québec, Canada
[2]Université du Québec à Trois-Rivières, Trois-Rivières, Québec, Canada
[3]Center for Northern Studies, Laval University, Québec, Québec, Canada

Received: 1 July 2015 – Accepted: 8 July 2015 – Published: 29 July 2015

Correspondence to: E. Godin (etienne.godin@gmail.com)

Published by Copernicus Publications on behalf of the European Geosciences Union.

Abstract

Low-centre polygonal terrain developing within gentle sloping surfaces and lowlands in the high Arctic have a potential to retain snowmelt water in their bowl-shaped centre and as such are considered high latitude wetlands. Such wetlands in the continuous permafrost regions have an important ecological role in an otherwise generally arid region. In the valley of the glacier C-79 on Bylot Island (Nunavut, Canada), thermal erosion gullies are rapidly eroding the permafrost along ice wedges affecting the integrity of the polygons by breaching and collapsing the surrounding rims. While intact polygons were characterized by a relative homogeneity (topography, snow cover, maximum active layer thaw depth, ground moisture content, vegetation cover), eroded polygons had a non-linear response for the same elements following their perturbation. The heterogeneous nature of disturbed terrains impacts active layer thickness, ground ice aggradation in the upper portion of permafrost, soil moisture and vegetation dynamics, carbon storage and terrestrial green-house gas emissions.

1 Introduction

Ice-wedge polygons as non-sorted patterned ground terrain type (Ballantyne, 2007) are widespread in the continuous permafrost zone characterizing the high Arctic (Black, 1976; Mackay and MacKay, 1974). High latitude valleys (Dostovalov and Popov, 1963) and more generally arctic lowlands are prone to the formation of low-centre polygon fields, which often typify a poor drainage and predominantly wet landscape (French, 2007; Zoltai and Tarnocai, 1975). Low centre polygons in arctic wetlands often develop ponds in their centres (Black, 1976) and are considered to have an important ecological role enabling suitable habitats for various macro species, either plants or animals (Gauthier et al., 1996, 2005, 2011, 2013; Jia et al., 2003; Massé et al., 2001; Myers-Smith et al., 2011; Woo and Young, 2012). Ponds and lakes commonly form in

BGD
12, 11797–11831, 2015

such polygonal wetlands, acting as carbon sinks when stable and GHG source when disturbance such as thermokarst occurs (Tranvik et al., 2009; Bouchard et al., 2015).

The main input for polygon water storage is snowmelt and the main output is evapotranspiration; the integrity of the polygon rims, the depth of active layer and the lateral flow within the active layer further contribute to the dynamic of the storage (Helbig et al., 2013). Distinct terrain units in a permafrost landscape (ex: polygons, ponds, hummocky terrain) can develop and co-exist over very short distances (few meters between each terrain units) with sensible differences among physical characteristics, such as the active layer depth, the ground temperature and the hydrological conditions (Boudreau and Rouse, 1995). A survey at the polygon scale demonstrated significant differences in the water balance, active layer depth and plant distribution among single polygons located in similar lowland mires but distant from each other by a few tens of kilometres (Minke et al., 2009) further identifying intra-site variability for almost identical terrain-unit. Another study satisfactorily demonstrated the variability in active layer depth in a non-disturbed and uniform 5 km^2 grid featured with high and low centre polygons (Gangodagamage et al., 2014).

Generally, permafrost disturbance and degradation exert a whole range of impacts on the affected area, such as but not limited to ecosystem shifts and consequent changes in topography and mass transfer (Jorgenson and Osterkamp, 2005). Disturbances in polygon fields such as by thermo-erosion gullying of ice wedges can occur very rapidly and with severe and immediate impacts on the terrain hydrology and ecological integrity (Fortier et al., 2007). On Bylot Island, one single gully eroded and breached hundreds of polygon ridges over a period of 14 years and clear changes were observed in polygon moisture and vegetation conditions (Godin et al., 2014; Perreault, 2012). Changes in cover and surface aspects are obvious near the gullied area and varies between eroded and intact polygons. Physical differences between a closed-rim polygon (intact) and an open one (due to gullying) located only a few meters apart can induce quite different plant communities in their respective centre in response to changing moisture and active layer conditions (Perreault et al., 2015). Vegetation changes in

BGD
12, 11797–11831, 2015

wetlands have direct implications on the food web as well: for instance in the Baffin area (and on Bylot Island), large avian herbivore populations rely on graminoids for support and the most adequate land unit (i.e. wetland) for this type of vegetation is quite restricted (Gauthier et al., 1996). Few detailed studies were conducted at the polygon scale with a specific focus on their thermal or moisture evolution through time while considering their micro-topography (Helbig et al., 2013; Minke et al., 2009). Questions remain as to how polygons are affected by permafrost degradation destroying the integrity of their ridges and what are the short and long term physical impacts following such a transformation.

This paper discusses the implications of polygon ridges erosion or polygon breach by gullying and how this changes the microtopography, near surface moisture conditions, active layer dynamics and vegetation distribution. This will be examined by comparing the aforementioned factors between undisturbed and eroded polygons, as a geomorphic unit.

2 Methods

2.1 Study site

The study site is located in the valley of the glacier C-79 (known as Qalikturvik valley) in the western part of Bylot Island in the eastern Canadian Arctic archipelago (73°09′ N 79°57′ W) (Fig. 1a). The 4 km wide per 17 km long valley (Fig. 1b) with glaciers at one end (C-79 and C-93) (Inland Water Branch, 1969) is drained via a proglacial braided river connected to the Navy Board Inlet sea branch. The pro-glacial river is bordered by a syngenetic ice-wedge polygons terrace. Several meter deep layers of loess and decomposed peat characterized the polygon terrace (Fig. 2) (Fortier and Allard, 2004). Polygons in the valley are either high centre or low centre; lakes and ponds are scattered over the terrace. Groups of high centre polygons are often surrounded by linear ponds that formed over ice wedges following collapse of polygon ridges (Bouchard

BGD
12, 11797–11831, 2015

et al., 2015). Several thermo-erosion gullies developed through the valley since 1958 and increased the hydrological connection from the valley walls to the braided river (Godin and Fortier, 2012a; Godin et al., 2014).

Climate normal (1981–2010) were recorded at the Pond Inlet Airport meteorological station at 62 m a.s.l. (Environment Canada, 2014) on Baffin Island, 85 km south east from the study site. Daily average air temperature was −14.6 °C and precipitation 189 mm (91 mm of rain) for this interval. A cross-correlation analysis revealed close correspondence between observations at the Pond Inlet Airport and those in the valley of the Glacier C-79 (Fortier and Allard, 2005; Gauthier et al., 2013). Daily average air temperature for the 1994–2013 interval at the study site was −14.5 °C (CEN, 2014).

Four polygons located nearby one well-developed and active gully labelled R08 (Godin et al., 2014) were instrumented (Fig. 2). Three of those polygons were partially breached by gully erosion, and the fourth was intact. The three polygons were initially breached in 1999 and early 2000's (Godin and Fortier, 2010b, 2012b) and stabilized since. Polygon geometry, temperature and moisture sensors model and experimental display are presented in Supplement 1.

2.2 Instruments, data acquisition and processing

2.2.1 Air and ground temperature

Polygons were drilled in 2012 using a modified portable permafrost core-drill system (Calmels et al., 2005) and the boreholes (BH), approximately one meter deep, were instrumented with a string of thermometers in polygons 331, 333, 573 (Fig. 3) and 563 (Fig. 4). Temperatures were recorded between summer 2012 and summer 2014. The 01 July 2013, a small 3 by 3 grid (±3 m × 3 m in size) in each polygon centres was measured using an active layer depth probe to validate the intra-polygonal variability and the thermal measurements of the monitored permafrost profiles. A string of thermistors installed in a borehole located in a low-centre polygon distant 2 km of the gully and connected to a logger (BYLOTPD, Fig. 2) recorded ground temperature on a profile

BGD
12, 11797–11831, 2015

between 2010 and summer 2013 at 10, 20, 30, 40, 80 cm (Allard et al., 2014). Air temperature was recorded onsite between 2010 and 2014 by two stations (BYLOSIL and BYLCAMP) from the SILA network (CEN, 2014). Precipitations during summer 2013 was obtained daily using a Hellmann Rain Gauge, compact version (CEN, 2014). All ground temperature data were graphed, analysed and interpreted using Golden Software's Surfer v8.

2.2.2 Ground moisture and cover

An array of five moisture sensors (TDR) were deployed in each studied polygon centres during summer 2013 to monitor the near-surface moisture regime (Figs. 3 and 4). Moisture sensor specifications are presented in Supplement 1. Volumetric water content (VWC, $m^3\,m^{-3}$) obtained using TDR sensors are presented in Supplement 2 in the annexes. Calibration of the recorded data was necessary (Czarnomski et al., 2005) due to the high organic content of the soils at the study site. The calibration was accomplished by saturating an instrumented (TDR) soil sample of known mass and volume while drying at air temperature, and weighing frequently, thus building a relation between the weight of the water in the sample and the signal in the moisture sensor. The equation derived from an exponential curve obtained from the logged data (R^2 = 0.97, n = 9), was applied to all moisture readings.

Snow conditions within and nearby the gully were obtained by time-lapse photography (daily, at noon during one year) between summer 2012 and summer 2013. The camera used was a Reconyx model PC-800 Hyperfire fixed on a tripod, with graduated poles deployed in the field of view within and nearby the gully for reference.

2.2.3 Plant characterization

As part of a larger study, each polygon was evaluated visually for vegetation cover using three randomly positioned 70 cm × 70 cm quadrats in July 2009 or 2010. Cover was evaluated visually with an abundance scale modified from Daubenmire (1959)

BGD
12, 11797–11831, 2015

for lichens and mosses and to species for vascular plants. Details on the methods are available in Perreault (2012). Vegetation results were compared with photographs obtained during the 2014 fieldwork to ascertain that sites were similar to 2010.

2.2.4 Active layer depth, degree-days and *n* factors

Air temperature has an important influence on ground temperature. Thawing degree day (DDT) and freezing degree days (DDF) are simple indexes used to calculate heat induction and extraction in a soil. A degree day is the difference between the mean daily temperature and 0 °C (Jumikis, 1977). The sum of the daily averages is then computed for a season, negative being DDF (freezing season) and positive DDT (thawing season).

Active layer depth at the end of the thawing season for a given site can be estimated using Stefan's equation modified for permafrost conditions (Brown et al., 2000; Jumikis, 1977):

$$Z = E\sqrt{\mathrm{DDT}_{\mathrm{air}}}$$

where Z represents the active layer depth, E the edaphic factors (or physical properties of the ground and its cover) and $\mathrm{DDT}_{\mathrm{air}}$ the sum of the average daily air temperature above 0 °C at the site (Brown et al., 2000; Shiklomanov et al., 2010; Woo et al., 2007). $\mathrm{DDT}_{\mathrm{air}}$ is provided by the nearby SILA stations (CEN, 2014).

Ratio between the $\mathrm{DDT}_{\mathrm{soil}}$ (sum of thawing degree day at soil surface) and $\mathrm{DDT}_{\mathrm{air}}$ provide the term n_{t} known as the thaw season n factor (Klene et al., 2001; Lunardini, 1978), as follows:

$$n_{\mathrm{t}} = \frac{\mathrm{DDT}_{\mathrm{soil}}}{\mathrm{DDT}_{\mathrm{air}}}$$

Similarly to n_{t}, the term n_{f} is used for freezing season n factor:

$$n_{\mathrm{f}} = \frac{\mathrm{DDF}_{\mathrm{soil}}}{\mathrm{DDF}_{\mathrm{air}}}$$

BGD
12, 11797–11831, 2015

where DDF_{soil} and DDF_{air} respectively stand for freezing degree day at ground surface and freezing degree day of air. DDF_{soil} and DDT_{soil} were provided by near surface sensors buried at 0.05 m in polygons 333 and 573 (BH location in Figs. 2 and 3).

Near surface thermal gradients were calculated for sites BYLOTPD (10–20 cm), 333 and 573 (5–20 cm) during August 2012 for summer and January 2013 for winter. Thermal gradient can be computed as:

$$i = \frac{T_s - T_b}{x}$$

where i is the thermal gradient ($^{\circ}C\,m^{-1}$), or the temperature change between two points in a medium, T_s and T_b are the temperature at surface and bottom and x the depth (length) of the layer considered in the measurement (Jumikis, 1977).

2.2.5 Statistics and landscape modelling

Quantitative analyses were performed with R (R Core Team, 2014); graphics with the ggplot2 module and PSI-Plot v9.5.

Site micro-topography was obtained using a Trimble VX station in survey; recoded spatial data was loaded and processed in ESRI's ArcGIS v10. High-resolution satellite images (GeoEYE) were used as background images for interpretation and analysis. Further details on geospatial sampling are available in Supplement 3.

3 Results

3.1 Ground moisture and cover

3.1.1 Winter dynamics

The snow cover during winter 2012–2013 began to accumulate in late September and was continuous until mid-May 2013. Polygons adjacent to the gully had at most 10 cm

BGD
12, 11797–11831, 2015

accumulation during the whole winter, most of the snow being blown away in the gully. In the depressions (gully), accumulations could either be absent or thicker than 1 m deep, depending of the channel sections. More generally, flat surfaces outside the gully acted as a source for snow and the gully channels as sinks (Pomeroy et al., 2007). Shallow snow cover exposing the ground to increased temperature variations during winter enabled more heat to be extracted from the ground and diminished the insulating role of snow, with a potential for a thinner maximum active layer depth. A slightly greater n_f was obtained at site 333 (n_f 2012–2013 = 0.99 and n_f 2013–2014 = 0.88) compared to 573 (n_f 2012–2013 = 0.99; n_f 2013–2014 = 0.88), indicating a thinner snow cover and larger heat extraction during winter. This result is strengthened by a higher DDF_{soil} value for 333 compared to 573 for both monitored winter (Table 1).

3.1.2 Summer dynamics

Snowmelt enabled the formation of a shallow pond each year in the centre of the intact polygon (573, Fig. 3). The pond disappeared late June to early July due to moisture evaporation and the lowering of the water table following propagation of the thaw front in the active layer. The moisture sensors installed in the centre of 573 (Fig. 5 and Supplement 2 for site 573) indicated a relative uniformity of the near surface moisture conditions inside the polygon. Moisture readings reacted in a similar direction and amplitude during rain events (Fig. 5, a clear augmentation of moisture during rains events E2, E3, E5 and E6 as shown by corresponding peaks) and during the progressive moisture decrease due to evapotranspiration and thaw depth increase. Values recorded for all moisture sensors in 573 polygon centre (Fig. 6, Supplement 2 for site 573) varied between 0.44 to 0.47 $m^3 m^{-3}$ VWC during early summer down to a minimum of 0.22 and 0.25 $m^3 m^{-3}$ VWC at the end of the logging interval. Thus moisture was consistent across time at the scale of this particular polygon centre and evolved uniformly to both inputs and outputs at all monitored locations inside this terrain unit.

Near surface ground moisture conditions evolution in eroded polygons 331, 333 (Fig. 3) and 563 (Fig. 4) was quite different than in the intact polygon 573 (Figs. 5 and

BGD
12, 11797–11831, 2015

6), when considering either the moisture balance of individual eroded polygons (intra-polygonal) and between polygons (inter-polygonal). Few locations (331-2 and 563-5) were similar to 573 during their evolution through the summer. The moisture at 331-2 varied between 0.29 to 0.43 $m^3 m^{-3}$ VWC, with an arithmetic mean of 0.35 ($\pm[1\sigma]0.04$). The moisture at 331-2 increased during rain events (Fig. 5, E3 and E5) and decreased following similar tendencies as the intact polygon. At the opposite, other locations (such as in Fig. 6, 333-2) were featured with nearly constant moisture through the summer, with very weak increases during precipitation events and a very subtle diminution of the moisture through the summer. Thaw depth was shallow ($\sim$ 20 cm) in at least some parts of the polygon 333 (Fig. 5, 333, red dashed line); mean thaw depth for 333 the 01 July 2013 was 19 cm (SD = 4). Sensors located 1.5 m each side of 333-2 (333-1 and 333-3) provided non-overlapping ranges for moisture – underlining a great variability under a short distance in this disturbed terrain unit.

3.2 Ground temperature and active layer thickness

Ground thermal regime monitoring obtained in an intact low-center polygon (BYLOTPD) between winter 2010 and summer 2013 provided maximum active layer depth of 56, 48.5, 52 and 40 cm for respectively 2010, 2011, 2012 and 2013 (BYLOTPD, Figs. 7, 8). When comparing ground thermal regime at the reference site against sites located near the gully, maximum active layer depths were within the same range for 2012 (331 = 47 cm, 563 = 44.5 cm and 573 = 52 cm) (Fig. 7). Active-layer depths were similar for those sites (except BYLOTPD) in 2013. On the other hand, 333 had a very shallow maximum ALD with 21 and 20.5 cm recorded for 2012 and 2013, less than half of the other monitored polygons, either intact or eroded. This was further validated by probing the active layer depth at several positions in the respective centres of the four polygons located nearby the gully during summer 2013. The intact polygon (573) had a lower intra-polygonal active layer depth variability within its grid compared to the other sites (thaw depth mean = 18 cm; SD = 2 cm the 01 July 2013).

BGD
12, 11797–11831, 2015

During summer of 2013, the n factor n_t was closer to the unity for 573 than 333 (respectively 1.02 and 1.06); thermal dynamics during summer were more complex than those of winter and albedo, nature of the cover, moisture and ground temperature need to be taken into consideration to precisely identify differences between sites. Thermal gradient were steeper during summer for 333 than for 573 (Table 3).

The n factor ratios n_f established for the sites indicate values closer to the unity during winter for 333 compared to 573. A n_f of 0.99 for 333 during 2012–2013 (Table 1) clearly suggesting a very low snow cover at the position. Thermal gradient for 333 was very steep at shallow depths with $-26 \pm 9\,^{\circ}\mathrm{C\,m^{-1}}$ (Table 3) during winter, reflecting the absence of a substantial snow cover; considerably lower than other intact sites either at Bylot Island or at other undisturbed sites. Thermal gradient in the literature during winter in the active layer or the near surface were similar for all sites except for 333.

Therefore the proximity of the gully and the consequent shallow snow cover in polygons nearby the eroded channels could impact how much heat can be extracted during winter, compared with an unaltered polygon (BYLOTPD) where local snow dynamics enabled thicker cover. Near-surface averaged maximum temperatures were generally cooler in the intact polygon (BYLOTPD, 3 °C) in 2012 compared with the other polygons as shown by the reddish colours delineating the 1 °C isolines in Fig. 8 (331, 333 = 8 °C, 563 = 5 °C, 573 = 10 °C).

The year 2012 had a warmer summer than 2013 and the winter 2012–2013 was warmer than the 2011–2012 winter (Table 2). The polygons located within a 1 km radius and those near the gully were exposed to similar DDT_{air}. Inter-polygonal differences in the active layer dynamics (e.g. moment of maximum ALD, maximum depth of the active layer, averaged values for near surface temperature) were due to polygon-specific surface characteristics (absence of snow cover during winter and vegetation, moisture during summer) impacting ground thermal dynamics on each respective sites.

BGD
12, 11797–11831, 2015

3.3 Vegetation in intact and eroded polygons

In 2010 and 2014, the centre of the intact wet polygon (573) was uniformly vegetated with typical wetland vegetation with low vascular plant diversity (i.e. wetland vegetation in Perreault et al., 2015 in this issue). Perreault (2012) measured a strong cover of living mosses (*Drepanochladus* sp. 53.3 % and *Polytricum* sp. 1.3 %) and *Carex aquatilis* (27.5 %), a sparse cover of *Dupontia fisheri* (0.5 %) and traces of *Pedicularis sudetica*, *Arctagrostis latifolia* and *Salix arctica* (Supplement 4). This polygon had a shallow pond in its centre from snowmelt until late June.

The three other polygons had a higher vascular plant diversity and less uniform vegetation with a mixture of wetland and mesic species typical of disturbed polygons (Perreault et al., 2015, this issue). Polygon 331 had 20 vascular plant species with the higher covers for wet habitat species with dried *Drepanochladus* sp. mosses (77.5 %), *Carex aquatilis* (6 %), *Dupontia fisheri* (3 %) *Eriophorum angustifolium* (2.5 %) and *Eriophorum scheuchzeri* (1.3 %) and traces for a number of typical mesic habitat species such as *Arctagrostis latifolia*, *Cerastium alpinum*, *Luzula confusa*, L. *arctica* and *Stellaria longipes*). Polygon 333 had part of its surface with bare-ground (2.5 %), a sign of disturbance, 42.7 % of dried mosses of wet habitat *Drepanochladus* sp. and 16 vascular plant species. Wet habitat species and mesic species shared the dominance with 21 % of *Eriophorum angustifolium* and 10.8 % of arctic willow (*Salix arctica*). Finally, polygon 563 with 11 vascular plant species was dominated by mesic habitat mosses *Aulacomnium* sp. (41.7 %) and vascular plants *Salix arctica* (19.3 %), *Arctagrostis latifolia* (3 %) and *Salix reticulata* (2.5 %). The typical wet species were not anymore present in this polygon.

BGD
12, 11797–11831, 2015

4 Discussion

4.1 Heterogeneity of eroded polygons

Eroded polygons adjacent to the gully were heterogeneous in their respective centres, with a thin snow cover, variable surface cover (vegetation distribution and cover), ground moisture conditions, active layer depths at the intra and inter-polygon scale. On the other hand, the undisturbed polygon (573) in this study was much more homogeneous compared to nearby eroded polygons, when considering the ground moisture tendencies, the active layer depth and the plant distribution. Pond formation in polygon 573 was observed in 2012 and 2013 and contributed to the hydrological recharge of this unit.

Basically, the heterogeneous character of the eroded polygons could depend on several elements, such as the length of the polygon contour adjacent to the gully (and incidentally its exposition to the gully), the ridge integrity (severity of its breaches) and the intrinsic potential to retain moisture in their centres, including the capacity to retain a snow cover during winter. Polygon 333 was among the most exposed to the gully and at the same time the most heterogeneous site in this study with notably very variable ground moisture levels and active layer depth, from excessively shallow up to comparable with other sites. These quite distinct physical traits compared to other eroded polygons and intact polygons were reinforced by the interconnection of many feedbacks. Simultaneously, the characteristics of an eroded polygon can be quite variable, showing either similarities to an intact polygon or differences as well. The contrasts between intact and eroded polygons were as follows:

1. Snow and insulation: The thinner snow cover enabled more heat to be extracted from the polygon centre during winter. Extreme negative winter thermal gradient of the near surface layer as observed in 333 with lows exceeding $-50\,^{\circ}\mathrm{C\,m^{-1}}$ underlining the direct effect of atmospheric conditions on the ground.

BGD
12, 11797–11831, 2015

2. Water balance and snow: snow is responsible for approximately half the yearly input in the water balance (Environment Canada, 2014), input which was likely displaced toward the topographical low (sink) due to gullying. As a result accumulations were reduced in disturbed polygon centre, therefore diminishing snowmelt input in polygons adjacent to sinks (Pomeroy et al., 2007). Water balance, lateral inflow and outflow: eroded polygon (333) was particularly influenced by nearby gullying conditions since 1999 (Godin and Fortier, 2012b) on two adjacent sides (south and west sides, Fig. 3). The polygon topography was transitioning towards the channel through a steep topographical gradient, in this case a 1.5 m vertical drop over a distance of 2 m on its west side. Surface flow following snowmelt and lateral inflow as the thaw depth increased (Helbig et al., 2013; Woo and Young, 2006) were drastically reduced in exposed polygons following the gully initiation and due to the local drainage reorganisation and runoff capture upstream (Godin and Fortier, 2010a; Godin et al., 2014). Further, lateral outflow from an eroded polygon was facilitated following a breach and ridge erosion, additionally aggravating the balance. Ground moisture changes: in disturbed polygons, a weak response (to rain events) could indicate the presence of a localized thicker thaw depth and a better soil infiltration capability for low moisture sites (563-2, 563-3) or a plain bad drainage in the thin ground thaw depth for moister sites (333-3, 333-4). This is a strong indication that the moisture in disturbed sites varies both at intra-polygon and inter-polygon scale. Otherwise the intact 573 had consistent near surface moisture in all its centre area.

3. Vegetation and cover: changes in moisture conditions inside the polygon forced changes on plant species distribution and abundance in its centre. From an uniformly cover composed of *Drepanochaldus* sp. and *Carex aquatilis* typical of an intact polygon (Billings and Peterson, 1980), a mosaic of *Eriophorum angustifolium*, *Salix arctica*, dryed *Carex* shoots, dried *Drepanochaldus* sp., a diversity of mesic species mixed with bared ground was found in the adjacent eroded polygons.

BGD
12, 11797–11831, 2015

4. Sparse prostrate tundra shrubs do not favour snow accumulation in the polygon centre (Pomeroy et al., 2006). Surface conditions characterized by such a cover following disturbance can accentuate the feedback effect of a thin snow cover due to the snow being blown in the nearby sink.

5. The sum of these conditions led to variable active layer depths some of those quite thin, with measured maximums of 20.5 and 21 cm in 2012 and 2013 (Fig. 7), when a few meter away in the two adjacent polygons the maximum active layer depth was twice deeper. As the moisture readily reached the base of the active layer, the local diminution of the depth of that layer implied the aggradation of that moisture as ice with the associated stored latent heat. Therefore thaw depth progression was closely connected with the sum of the DDT_{air} for intact polygons, which is uncertain with an eroded site.

6. The thinning of the active layer further implied local ground ice, carbon and nutrient fixation due to freezing following permafrost aggradation, but very locally in 333.

All breached polygon centres in this study were similarly variable within their physical properties as 333 but to a lesser degree.

4.2 Variability: implication

Following the glacier retreat in the valley (Allard, 1996), a syngenetic low-centre polygon terrace initiated over the valley floor, as a relatively continuous, low topographic gradient surface. In this particular valley, the terrace on the valley floor progressively evolved during the following millenniums; lakes were formed and some were drained, pingos were formed and became inactive. Especially, groups of polygon ridges were gradually eroded and evolved towards high-centre polygons; other stayed low-centre to this day.

BGD
12, 11797–11831, 2015

Polygon ridges erosion leading to high centre polygons affects several sections of the terrace in the valley over an extended period of time, several centuries at least, as denoted in a previous study in the same valley (Ellis et al., 2008). On the other hand, thermo-erosion gullying is a process occurring very suddenly and rapidly (Fortier et al., 2007) and is distinct from wedge erosion leading to high-centre polygons. Feedbacks following the initiation of a gully such as the drainage network rearrangement often accelerate the gullying during the first stages (Sidorchuk, 1999). Simultaneously, the watershed hydrological network reacts and adapts to this new geomorphology transforming a continuous quasi-flat surface to an incised terrace enabling channelized flow (sinkholes, channels, depressions).

Transition interval following a sudden change of conditions for a geosystem therefore starts with rapid changes which progressively diminish as a new equilibrium is in the process of being established. Similarly to the Illisarvik lake experiment following the drainage, a new state of equilibrium followed the initial perturbation (Mackay and Burn, 2002a, b). Polygons in the current study were in transition toward the new equilibrium – changes in surface conditions caused non-linear fluctuations in the active layer depth, moisture content and plant species distribution and occurrence. The significant amount of dried plants (e.g. dead mosses and dead *Carex aquatilis*) in 333 and the higher vascular plant diversity compared with the nearby intact polygon support the idea of transition (Perreault et al., 2015), where heterogeneity in abiotic conditions offers opportunities for mesic plant species. Polygon 563 could indicate an example of a new equilibrium state following rim erosion: it was located in a stabilized section of the gully where there was no runoff input, where ground thermal regime was similar to 573, with intermediate moisture levels and a vegetation cover somewhat distinct from other sites (Supplement 4). In any cases, the breached polygons definitely will not return to their pre-erosion state.

Considering the polygon terrace as a whole, it evolved from the initial cracking and syngenetic evolution of ice-wedge toward low-centre polygon. From that state, sections of the landscape either kept evolving as low centre polygons or degraded progres-

BGD
12, 11797–11831, 2015

sively toward high-centre polygon. This enabled distinct landforms (high-centre and low-centre polygons) stemming from a common origin and geomorphological context to simultaneously co-evolve, with gullying being an erosion risk for low-centre polygons exclusively in this case. It remains to be seen how these rapid changes to drainage conditions impact the opportunity for low-centre polygons to evolve to high-centre toward the watershed outlet (downstream). Further, polygons which were suddenly breached reveal non-linear intra-polygonal variability. Old stabilized gully sections (in the R08 gully or others in the valley) were vegetated as a result of erosion-stabilization, with plants adapted to gully slope conditions. (Fortier et al., 2006) used the polygon centres as proxy for paleo-environmental analysis and one of the conclusions was that polygon moisture oscillate, at a millennium time scale, depending on the climate state (wetter, dryer): climate was wetter between 250 and 1750 BP. At the landscape scale and short term, gullying could force a dryer state for eroded polygons during a climatic wet period, keeping this form dryer than intact polygons for the same climate conditions. Additionally, polygons similarly affected during a dry period could further aggravate surface conditions in an already dry climate period. This represents two vectors for erosion, at two distinct spatial and time scales, having a simultaneous role in continuous permafrost landscape evolution.

5 Conclusions

Intact low centre polygons evolving in a terrace covering a valley floor in the western section of Bylot Island in the Canadian High Arctic were homogenous in their centre and between each other. Polygons with ridges breached by thermal erosion gullying were comparatively heterogeneous, with variable ground moisture retention capacity, active layer depth, vegetation cover and distribution: intact and breached polygons located a few meter apart presented contrasting centres characteristics between each unit. At a landscape scale, low centre polygons as an initial equilibrium stage can either evolve progressively toward high centre polygons zones, or change very rapidly

BGD
12, 11797–11831, 2015

after being breached due to thermal erosion. Breached polygons will establish a new equilibrium state after local erosion stabilize – with a mesic environment and dryer surface, which conditions could be further aggravate in the event of a dryer climate period.

The Supplement related to this article is available online at doi:10.5194/bgd-12-11797-2015-supplement.

Acknowledgements. We are very thankful to Gilles Gauthier and his team (Center for Northern Studies) for welcoming us to his research station and providing access to field logistics. Our project was made possible due to the financial/field support by the following organizations: Parks Canada Staff (Sirmilik), the Polar Continental Shelf Program, the Northern Scientific Training Program by the Canadian Polar Commission, ArcticNet, the ArcticWOLVES IPY program, NSERC, NSERC-ADAPT, NSERC-Discovery, FRQNT, the W. Garfield Weston Foundation and the Département de Géographie de l'Université de Montréal.

We are extremely grateful to Naïm Perreault, Stéphanie Coulombe, Laurent Lamarque, Michel Paquette, Audrey Veillette, Dr. Michel Allard, Sabine Veuille, Gabrielle Létourneau, Laurent Gosselin and Josée Turcotte for their help in the field, discussions on methods, concepts and preparation of the manuscript.

References

Allard, M.: Geomorphological changes and permafrost dynamics: key factors in changing arctic ecosystems. An example from Bylot Island, Nunavut, Canada, Geosci. Can., 23, 205–212, available at: https://journals.lib.unb.ca/index.php/GC/article/viewArticle/3916, 1996. 11811

Allard, M. and Kasper, J. N.: Temperature conditions for ice wedge cracking: field measurements from Salluit, northern Québec, in: Proceedings of the Seventh International Conference on Permafrost, Yellowknife, Canada, Collection Nordicana, Centre d'études nordiques, Université Laval, Québec, 23–27 June 1998, Yellowknife, NWT, Canada, 5–12, 1998. 11823

BGD
12, 11797–11831, 2015

Allard, M., Sarrazin, D., and L'Hérault, E.: Borehole monitoring temperatures in northeastern Canada, v. 1.2 (1988–2014), Nordicana D8, doi:10.5885/45291SL-34F28A9491014AFD, 2014. 11802, 11825

Ballantyne, C. K.: Periglacial Landforms | Patterned Ground, Elsevier, Oxford, 2182–2191, doi:10.1016/B0-44-452747-8/00107-1, 2007. 11798

Billings, W. D. and Peterson, K. M.: Vegetational change and ice-wedge polygons through the thaw-lake cycle in Arctic Alaska, Arctic Alpine Res., 12, 413–432, doi:10.2307/1550492, 1980. 11810

Black, R. F.: Periglacial features indicative of permafrost: ice and soil wedges, Quaternary Res., 6, 3–26, doi:10.1016/0033-5894(76)90037-5, 1976. 11798

Bouchard, F., Laurion, I., Preskienis, V., Fortier, D., Xu, X., and Whiticar, M. J.: Modern to millennium-old greenhouse gases emitted from freshwater ecosystems of the eastern Canadian Arctic, Biogeosciences Discuss., 12, 11661–11705, doi:10.5194/bgd-12-11661-2015, 2015. 11799, 11800

Boudreau, L. D. and Rouse, W. R.: The role of individual terrain units in the water balance of wetland tundra, Clim. Res., 5, 31–47, 1995. 11799

Brown, J., Hinkel, K. M., and Nelson, F. E.: The circumpolar active layer monitoring (CALM) program: research designs and initial results 1, Polar Geography, 24, 166–258, doi:10.1080/10889370009377698, 2000. 11803

Calmels, F., Gagnon, O., and Allard, M.: A portable earth-drill system for permafrost studies, Permafrost Periglac., 16, 311–315, doi:10.1002/ppp.529, 2005. 11801

CEN: Environmental data from Bylot Island in Nunavut, Canada, v. 1.4 (1992–2014), Nordicana D2, doi:10.5885/45039SL-EE76C1BDAADC4890, 2014. 11801, 11802, 11803, 11821, 11822, 11825

Czarnomski, N. M., Moore, G. W., Pypker, T. G., Licata, J., and Bond, B. J.: Precision and accuracy of three alternative instruments for measuring soil water content in two forest soils of the Pacific Northwest, Can. J. Forest Res., 35, 1867–1876, doi:10.1139/x05-121, 2005. 11802

Daubenmire, R.: A canopy-coverage method of vegetational analysis, Northwest Sci., 33, 43–64, 1959. 11802

Dostovalov, B. N. and Popov, A. I.: Polygonal systems of ice-wedges and conditions of their development, in: Proceedings of the First International Conference on Permafrost, vol. 1, Na-

BGD
12, 11797–11831, 2015

tional Academy of Sciences-National Research Council, 11–15 November 1963, Lafayette, Indiana, USA, 102–105, 1963. 11798
Ellis, C. J., Rochefort, L., Gauthier, G., and Pienitz, R.: Paleoecological evidence for transitions between contrasting landforms in a polygon-patterned high Arctic wetland, Arct. Antarct. Alp. Res., 40, 624–637, doi:10.1657/1523-0430(07-059)[ELLIS]2.0.CO;2, 2008. 11812
Environment Canada: Canadian Climate Normals, 1981–2010, Pond Inlet, available at: http://climate.weather.gc.ca/climate_normals/ (last access: 24 July 2015), 2014. 11801, 11810
Fortier, D. and Allard, M.: Late Holocene syngenetic ice-wedge polygons development, Bylot Island, Canadian Arctic Archipelago, Can. J. Earth Sci., 41, 997–1012, doi:10.1139/e04-031, 2004. 11800
Fortier, D. and Allard, M.: Frost-cracking conditions, Bylot Island, Eastern Canadian Arctic Archipelago, Permafrost Periglac., 16, 145–161, doi:10.1002/ppp.504, 2005. 11801, 11823
Fortier, D., Allard, M., and Pivot, F.: A late-Holocene record of loess deposition in ice-wedge polygons reflecting wind activity and ground moisture conditions, Bylot Island, eastern Canadian Arctic, Holocene, 16, 635–646, doi:10.1191/0959683606hl960rp, 2006. 11813
Fortier, D., Allard, M., and Shur, Y.: Observation of rapid drainage system development by thermal erosion of ice wedges on Bylot island, Canadian Arctic Archipelago, Permafrost Periglac., 18, 229–243, 2007. 11799, 11812
French, H. M.: The Periglacial Environment, 3rd edn., John Wiley and Sons, Chichester, England, Hoboken, NJ, 2007. 11798
Gangodagamage, C., Rowland, J. C., Hubbard, S. S., Brumby, S. P., Liljedahl, A. K., Wainwright, H., Wilson, C. J., Altmann, G. L., Dafflon, B., Peterson, J., Ulrich, C., Tweedie, C. E., and Wullschleger, S. D.: Extrapolating active layer thickness measurements across Arctic polygonal terrain using LiDAR and NDVI data sets, Water Resour. Res., 50, 6339–6357, doi:10.1002/2013WR014283, 2014. 11799
Gauthier, G., Rochefort, L., and Reed, A.: The exploitation of wetland ecosystems by herbivores on Bylot island, Geosci. Can., 23, 253–259, 1996. 11798, 11800
Gauthier, G., Giroux, J.-F., Reed, A., Béchet, A., and Bélanger, L.: Interactions between land use, habitat use, and population increase in greater snow geese: what are the consequences for natural wetlands?, Glob. Change Biol., 11, 856–868, doi:10.1111/j.1365-2486.2005.00944.x, 2005. 11798

BGD
12, 11797–11831, 2015

Gauthier, G., Berteaux, D., Bety, J., Tarroux, A., Therrien, J. F., McKinnon, L., Legagneux, P., and Cadieux, M. C.: The tundra food web of Bylot Island in a changing climate and the role of exchanges between ecosystems, Ecoscience, 18, 223–235, 2011. 11798

Gauthier, G., Béty, J., Cadieux, M.-C., Legagneux, P., Doiron, M., Chevallier, C., Lai, S., Tarroux, A., and Berteaux, D.: Long-term monitoring at multiple trophic levels suggests heterogeneity in responses to climate change in the Canadian Arctic tundra, Philos. T. R. Soc. B, 368, 20120482, doi:10.1098/rstb.2012.0482, 2013. 11798, 11801

Godin, E. and Fortier, D.: Distribution and local hydrographic impact of rapid permafrost degradation by thermo-erosion and gullying of ice-wedge polygons in glacier valley C-79 on Bylot Island, Nunavut, Canada, Abstract C31A-0490 presented at 2010 Fall Meeting, AGU, San Francisco, Calif., 13–17 December, 2010a. 11810

Godin, E. and Fortier, D.: Geomorphology of thermo-erosion gullies – case study from Bylot Island, Nunavut, Canada, in: Proceedings of the Sixty-Third Canadian Geotechnical Conference & Sixth Canadian Permafrost Conference, vol. 1, Calgary, Canada, 1540–1547, 12–16 September 2010, Calgary, Alberta, Canada, available at: http://pubs.aina.ucalgary.ca/cpc/CPC6-1540.pdf, 2010b. 11801

Godin, E. and Fortier, D.: Fine-scale spatio-temporal monitoring of multiple thermo-erosion gully development on Bylot Island, Eastern Canadian Archipelago, in: Proceedings of the Tenth International Conference on Permafrost, vol. 1, edited by: Hinkel, K. M., The Northern Publisher Salekhard, 125–130, 25–29 June 2012, Salekhard, Russia, available at: http://ipa.arcticportal.org/meetings/international-conferences (last access: 24 July 2015), 2012a. 11801

Godin, E. and Fortier, D.: Geomorphology of a thermo-erosion gully, Bylot Island, Nunavut, Canada, Can. J. Earth Sci., 49, 979–986, doi:10.1139/e2012-015, 2012b. 11801, 11810

Godin, E., Fortier, D., and Coulombe, S.: Effects of thermo-erosion gullying on hydrologic flow networks, discharge and soil loss, Environ. Res. Lett., 9, 105010, doi:10.1088/1748-9326/9/10/105010, 2014. 11799, 11801, 11810

Helbig, M., Boike, J., Langer, M., Schreiber, P., Runkle, B. K., and Kutzbach, L.: Spatial and seasonal variability of polygonal tundra water balance: Lena River Delta, northern Siberia (Russia), Hydrogeol. J., 21, 133–147, doi:10.1007/s10040-012-0933-4, 2013. 11799, 11800, 11810

BGD
12, 11797–11831, 2015

Hinzman, L. D., Kane, D. L., Gieck, R. E., and Everett, K. R.: Hydrologic and thermal properties of the active layer in the Alaskan Arctic, Cold Reg. Sci. Technol., 19, 95–110, doi:10.1016/0165-232X(91)90001-W, 1991. 11823

Inland Water Branch: Bylot Island Glacier Inventory: Area 46201, Department of Energy, Mines and Resources, Ottawa, 76 pp., 1969. 11800

Jia, G. J., Epstein, H. E., and Walker, D. A.: Greening of arctic Alaska, 1981–2001, Geophys. Res. Lett., 30, 2067, doi:10.1029/2003GL018268, 2003. 11798

Jorgenson, M. T. and Osterkamp, T. E.: Response of boreal ecosystems to varying modes of permafrost degradation, Can. J. Forest Res., 35, 2100–2111, doi:10.1139/x05-153, 2005. 11799

Jumikis, A. R.: Thermal Geotechnics, Rutgers University Press, New Brunswick, N. J., 1977. 11803, 11804

Klene, A. E., Nelson, F. E., Shiklomanov, N. I., and Hinkel, K. M.: The n-factor in natural landscaper: variability of air and soil-surface temperatures, Kuparuk River basin, Alaska, USA, Arct. Antarct. Alp. Res., 33, 140–148, doi:10.2307/1552214, 2001. 11803

Lunardini, V. J.: Theory of n-factors and correlation of data, in: Proceedings of the Third International Conference on Permafrost, 10–13 July 1978, Edmonton, Alberta, Canada, vol. 1, 40–46, 1978. 11803

Mackay, J. and MacKay, D.: Snow cover and ground temperatures, Garry Island, N. W. T, Arctic, 27, 287–296, 1974. 11798

Mackay, J. R.: The first 7 years (1978–1985) of ice wedge growth, Illisarvik experimental drained lake site, western Arctic coast, Can. J. Earth Sci., 23, 1782–1795, doi:10.1139/e86-164, 1986. 11823

Mackay, J. R. and Burn, C. R.: The first 20 years (1978–1979 to 1998–1999) of active-layer development, Illisarvik experimental drained lake site, western Arctic coast, Canada, Can. J. Earth Sci., 39, 1657–1674, doi:10.1139/e02-068, 2002a. 11812

Mackay, J. R. and Burn, C. R.: The first 20 years (1978–1979 to 1998–1999) of ice-wedge growth at the Illisarvik experimental drained lake site, western Arctic coast, Canada, Can. J. Earth Sci., 39, 95–111, doi:10.1139/e01-048, 2002b. 11812

Massé, H., Rochefort, L., and Gauthier, G.: Carrying capacity of wetland habitats used by breeding greater snow geese, The Journal of Wildlife Management, 65, 271–281, doi:10.2307/3802906, 2001. 11798

BGD
12, 11797–11831, 2015

Minke, M., Donner, N., Karpov, N., de Klerk, P., and Joosten, H.: Patterns in vegetation composition, surface height and thaw depth in polygon mires in the Yakutian Arctic (NE Siberia): a microtopographical characterisation of the active layer, Permafrost Periglac., 20, 357–368, doi:10.1002/ppp.663, 2009. 11799, 11800

Myers-Smith, I. H., Forbes, B. C., Wilmking, M., Hallinger, M., Lantz, T., Blok, D., Tape, K. D., Macias-Fauria, M., Sass-Klaassen, U., Lévesque, E., Boudreau, S., Ropars, P., Hermanutz, L., Trant, A., Collier, L. S., Weijers, S., Rozema, J., Rayback, S. A., Schmidt, N. M., Schaepman-Strub, G., Wipf, S., Rixen, C., Ménard, C. B., Venn, S., Goetz, S., Andreu-Hayles, L., Elmendorf, S., Ravolainen, V., Welker, J., Grogan, P., Epstein, H. E., and Hik, D. S.: Shrub expansion in tundra ecosystems: dynamics, impacts and research priorities, Environ. Res. Lett., 6, 045509, doi:10.1088/1748-9326/6/4/045509, 2011. 11798

Perreault, N.: Impact of permafrost gullying on wetland habitat, Bylot Island, Nunavut, Canada, M.S. thesis, Thesis, UQTR, Trois-Rivières, Québec, Canada, 2012. 11799, 11803, 11808

Perreault, N., Levesque, E., Fortier, D., and Lamarque, L. J.: Thermo-erosion gullies boost the transition from wet to mesic vegetation, Biogeosciences Disc., 2015. 11799, 11808, 11812

Pomeroy, J. W., Bewley, D. S., Essery, R. L. H., Hedstrom, N. R., Link, T., Granger, R. J., Sicart, J. E., Ellis, C. R., and Janowicz, J. R.: Shrub tundra snowmelt, Hydrol. Process., 20, 923–941, doi:10.1002/hyp.6124, 2006. 11811

Pomeroy, J. W., Gray, D. M., Brown, T., Hedstrom, N. R., Quinton, W. L., Granger, R. J., and Carey, S. K.: The cold regions hydrological model: a platform for basing process representation and model structure on physical evidence, Hydrol. Process., 21, 2650–2667, doi:10.1002/hyp.6787, 2007. 11805, 11810

R Core Team: R: a Language and Environment for Statistical Computing, R Foundation for Statistical Computing, Vienna, Austria, available at: http://www.R-project.org/ (last access: 24 July 2015), 2014. 11804

Shiklomanov, N. I., Streletskiy, D. A., Nelson, F. E., Hollister, R. D., Romanovsky, V. E., Tweedie, C. E., Bockheim, J. G., and Brown, J.: Decadal variations of active-layer thickness in moisture-controlled landscapes, Barrow, Alaska, J. Geophys. Res.-Biogeo., 115, G00I04, doi:10.1029/2009JG001248, 2010. 11803

Sidorchuk, A.: Dynamic and static models of gully erosion, Catena, 37, 401–414, doi:10.1016/s0341-8162(99)00029-6, 1999. 11812

Tranvik, L. J., Downing, J. A., Cotner, J. B., Loiselle, S. A., Striegl, R. G., Ballatore, T. J., Dillon, P., Finlay, K., Fortino, K., Knoll, L. B., Kortelainen, P. L., Kutser, T., Larsen, S., Laurion, I.,

BGD
12, 11797–11831, 2015

Leech, D. M., McCallister, S. L., McKnight, D. M., Melack, J. M., Overholt, E., Porter, J. A., Prairie, Y., Renwick, W. H., Roland, F., Sherman, B. S., Schindler, D. W., Sobek, S., Tremblay, A., Vanni, M. J., Verschoor, A. M., von Wachenfeldt, E., and Weyhenmeyer, G. A.: Lakes and reservoirs as regulators of carbon cycling and climate, Limnol. Oceanogr., 54, 2298–2314, doi:10.4319/lo.2009.54.6_part_2.2298, 2009. 11799

Watanabe, T., Matsuoka, N., and Christiansen, H. H.: Ice- and soil-wedge dynamics in the Kapp Linné Area, Svalbard, investigated by two- and three-dimensional GPR and ground thermal and acceleration regimes, Permafrost Periglac., 24, 39–55, doi:10.1002/ppp.1767, 2013. 11823

Woo, M. K. and Young, K.: Wetlands of the Canadian Arctic, book section 229, in: Encyclopedia of Earth Sciences Series, Springer Netherlands, 902–914, doi:10.1007/978-1-4020-4410-6_229, 2012. 11798

Woo, M. K. and Young, K. L.: High Arctic wetlands: their occurrence, hydrological characteristics and sustainability, J. Hydrol., 320, 432–450, doi:10.1016/j.jhydrol.2005.07.025, 2006. 11810

Woo, M.-K., Mollinga, M., and Smith, S. L.: Climate warming and active layer thaw in the boreal and tundra environments of the Mackenzie Valley, Can. J. Earth Sci., 44, 733–743, doi:10.1139/e06-121, 2007. 11803

Zoltai, S. C. and Tarnocai, C.: Perennially Frozen peatlands in the Western Arctic and subarctic of Canada, Can. J. Earth Sci., 12, 28–43, doi:10.1139/e75-004, 1975. 11798

BGD
12, 11797–11831, 2015

Table 1. Degree days of freeze (DDF_{air}) as recorded by the on-site meteorological stations, between 2010 and 2014 (CEN, 2014), and DDF_{soil} for 333 and 573 (winter 2012–2013 and 2013–2014). The length of the thawing season is indicated for each measured unit under their respective *n* day column.

Winter	*n* day	DDF_{air}	*n* day	DDF_{soil} 573	*n* day	DDF_{soil} 333
2010–2011	256	5331				
2011–2012	262	5343				
2012–2013	271	4922	260	4698	260	4846
2013–2014	272	5674	265	4834	256	5015

BGD
12, 11797–11831, 2015

Table 2. Degree days of thaw (DDT_{air}) as recorded by the on-site meteorological stations, between 2010 and 2014 (CEN, 2014), and DDT_{soil} for 333 and 573 (summer 2013). The length of the thawing season is indicated for each measured unit under their respective *n* day column.

Summer	*n* day	DDT_{air}	*n* day	DDT_{soil} 573	*n* day	DDT_{soil} 333
2010	114	526				
2011	97	556				
2012	96	495				
2013	98	450	92	459	93	476

BGD
12, 11797–11831, 2015

Table 3. Thermal gradients reported from the literature (as reference) and from sites in this study (333, 573). The gradient i °C m^{-1}, the depth, the season, the location and the source are mentioned. Winter thermal gradient were common while spring/summer gradients sparser.

i, °C m^{-1}	Depth (m)	Season	Location	Source
2.5 to 11	0–0.5	Spring	Bylot Isl., NU, CA	Fortier and Allard (2005)
$-10.9 \pm (-3.9 - 18.9]$	0–0.4	Winter	Bylot Isl., NU, CA	Fortier and Allard (2005)
−15 to −10	0–0.45	Winter	Illisarvik LK, NWT, CA	Mackay (1986)
10	Near surf.	Winter	Salluit, QC, CA	Allard and Kasper (1998)
Less than −15	0–0.25	Winter	Svalbard, NO	Watanabe et al. (2013)
−15 to −7	0.25–0.75	Winter	Svalbard, NO	Watanabe et al. (2013)
0.5 to 5	0–0.4	Summer	Brooks Range, AK, USA	Hinzman et al. (1991)
−8 to −1	0–0.4	Winter	Brooks Range, AK, USA	Hinzman et al. (1991)
$2 \pm 1(1\sigma)$	0.1–0.2	Summer	Bylot Isl., NU, CA	BYLOTPD (this study)
$-13 \pm 3(1\sigma)$	0.1–0.2	Winter	Bylot Isl., NU, CA	BYLOTPD (this study)
$-26 \pm 9(1\sigma)$	0.05–0.2	Winter	Bylot Isl., NU, CA	333 (this study)
$39 \pm 10(1\sigma)$	0.05–0.2	Summer	Bylot Isl., NU, CA	333 (this study)
$-8 \pm 3(1\sigma)$	0.05–0.2	Winter	Bylot Isl., NU, CA	573 (this study)
$19 \pm 6(1\sigma)$	0.05–0.2	Summer	Bylot Isl., NU, CA	573 (this study)

BGD
12, 11797–11831, 2015

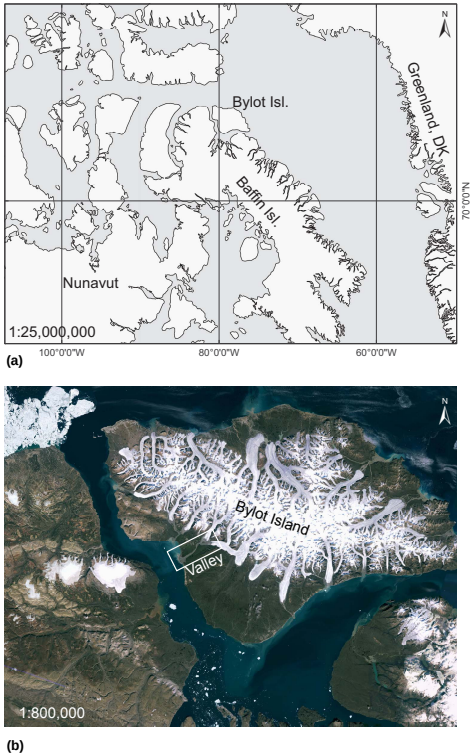

Figure 1. The study site is on Bylot Island in the Canadian Arctic archipelago (73°09′ N 79°57′ W), north of Baffin Island **(a)**. The valley of the glacier C-79 is located in the southwestern section of the island **(b)** (background: NRCan Landsat-7 orthorectified mosaic, 03 August 2010).

BGD
12, 11797–11831, 2015

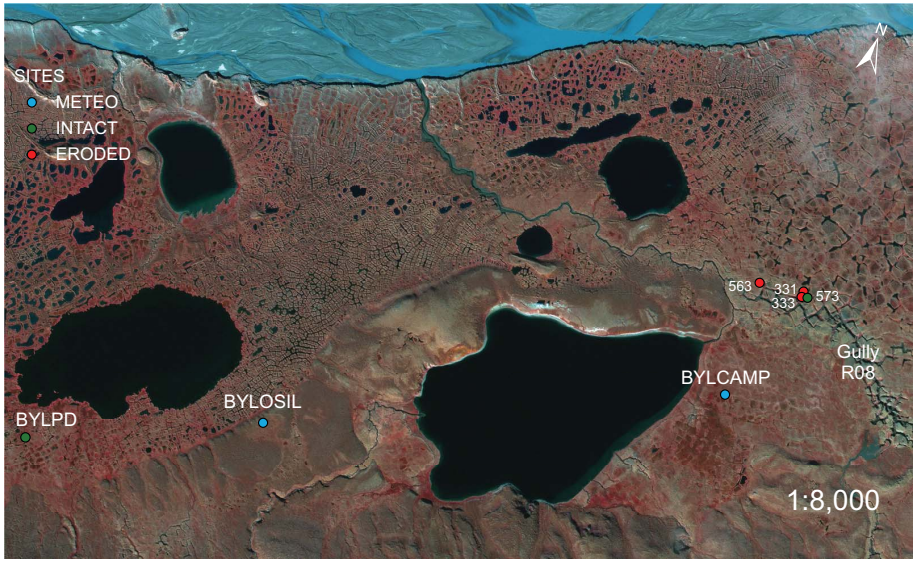

Figure 2. The location of the stations at study site; map background is a GEO-Eye false colour satellite image (Near Infra-Red, Red, Green) obtained the 02 September 2010. BYLOSIL and BYLCAMP are meteorological stations part of the SILA network (CEN, 2014). BYLOTPD is a reference ground temperature monitoring site installed in a low-center polygon (Allard et al., 2014). The gully R08 is located on the right side of the image, N-E of the lake. Stations 331, 333, 563 and 573 are located near the gully margin.

BGD
12, 11797–11831, 2015

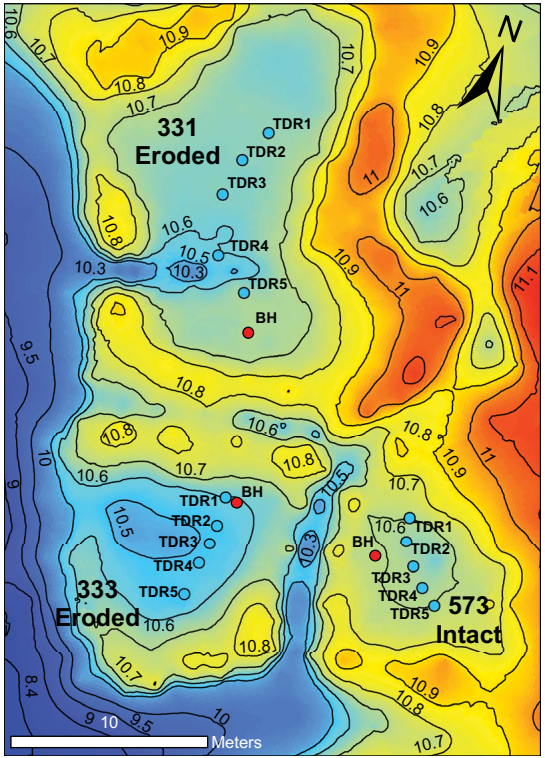

Figure 3. Digital elevation model of sites 331, 333 and 573. Altitudinal isolines contours were digitized on the figure at each 0.1 m. A gully channel (deep blue) initiated in 1999 near polygons; rims (yellow and orange) delineate polygon contours; light blue indicate a breached polygon (331 and 333). 573 ridge contouring the polygon is intact. The gully channel floor (dark blue) is approximately 2 m lower than nearby polygons rims at this position. Boreholes equipped with a string of thermometers (BH in the figure) are identified in red in each polygons, and moisture sensors in blue (TDR in the figure).

BGD
12, 11797–11831, 2015

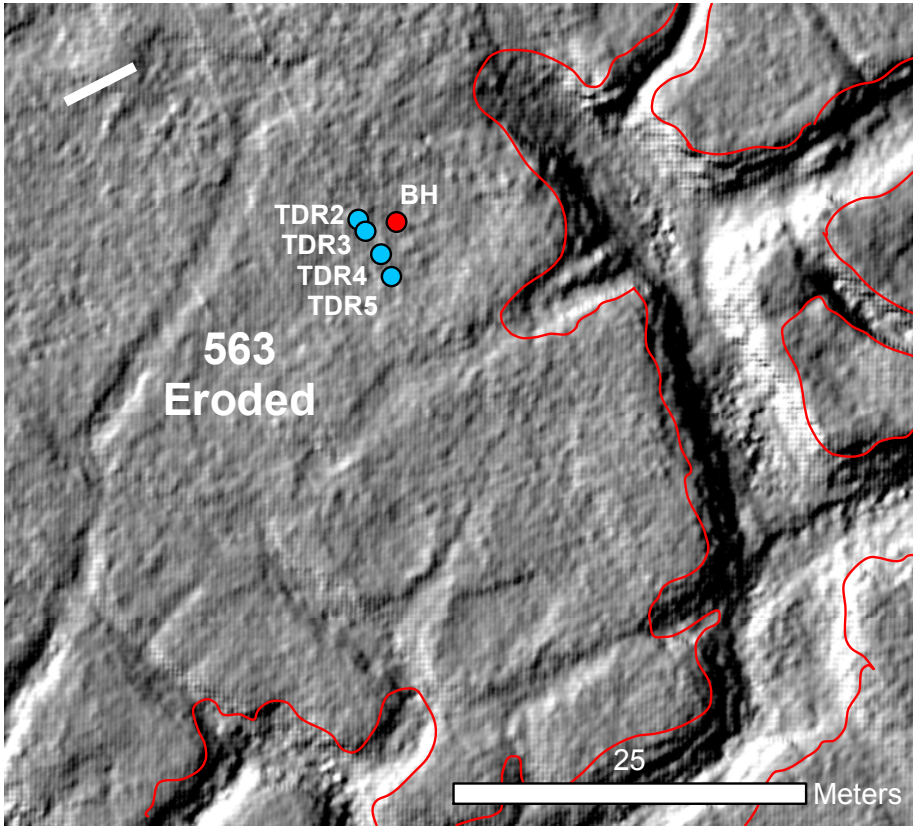

Figure 4. The background of this image is a high resolution photo-mosaic displaying the terrain in the area near polygon 563, polygon breached to the south and to the east (mosaic obtained in 2014). The borehole is indicated in red (BH) and moisture sensors positions in blue (TDR). Polygon 563 is breached to the south and connected to the gully channel to the east (gully contours in red).

BGD
12, 11797–11831, 2015

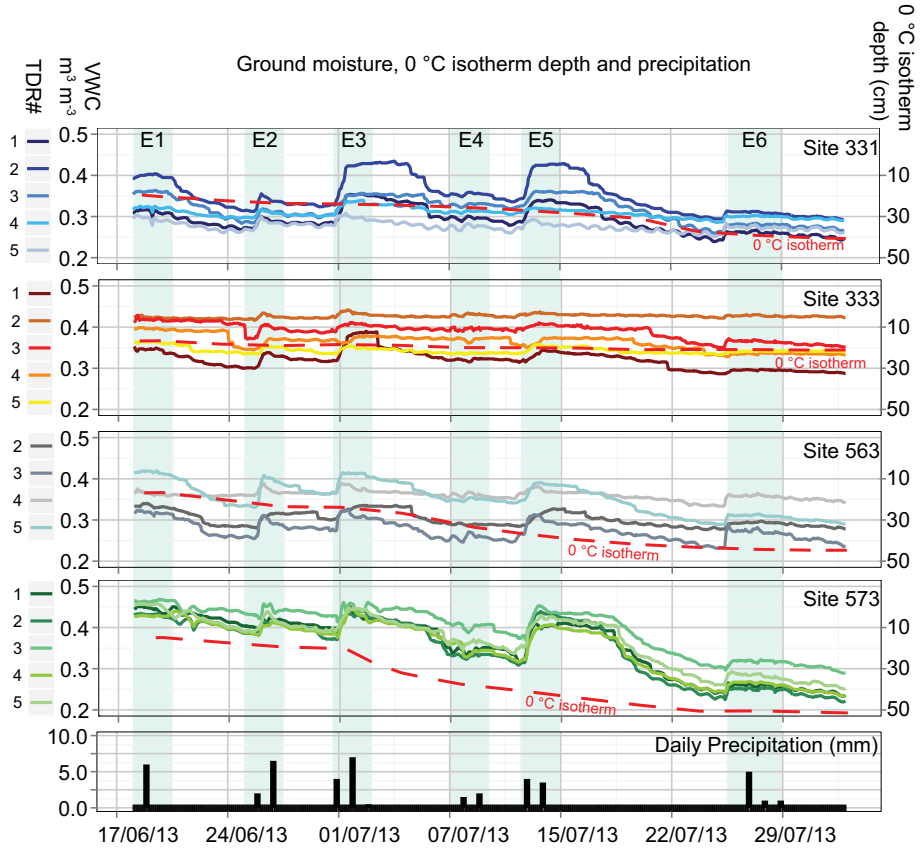

Figure 5. Moisture readings for the near surface of sites 331, 333, 563 and 573 during summer 2013 (Figs. 3 and 4). Daily precipitation readings indicated 6 rain events through the summer, identified in the figure E1 to E6. Propagation of the thaw front in the active layer evolution is identified as the 0˚C isoline for each sites – moisture levels decreased following active layer depth for all sites except 333.

BGD
12, 11797–11831, 2015

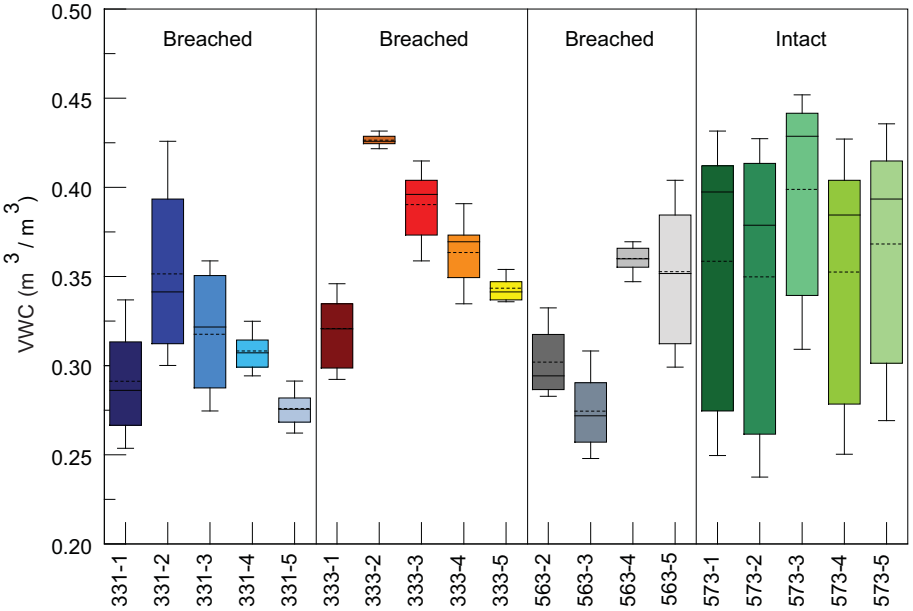

Figure 6. Variability of moisture conditions during summer 2013 (VWC $m^3 m^{-3}$), per polygon, for each sensor. Box plot colour map in the figure is the same than in Fig. 5.

BGD
12, 11797–11831, 2015

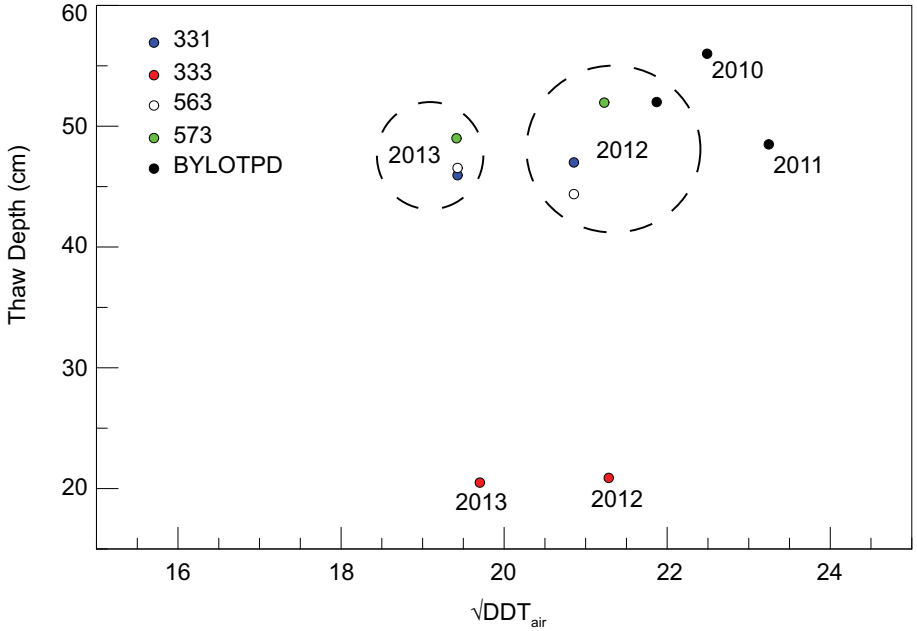

Figure 7. Maximum active layer thaw-depth related to the square root sum of degree day of thaw (air) for sites in the valley between 2010 and 2013. The relation between those two variables for the sites was similar for most locations except 333. The reference site BYLOTPD varied weakly from year to year. Sites measured in 2012 were exposed to more DDT than in 2013, but the tendency was not reflected clearly on the maximum active layer depth – possibly implying varying edaphic factors between both years. 333's depth was virtually the same between 2012 and 2013.

BGD
12, 11797–11831, 2015

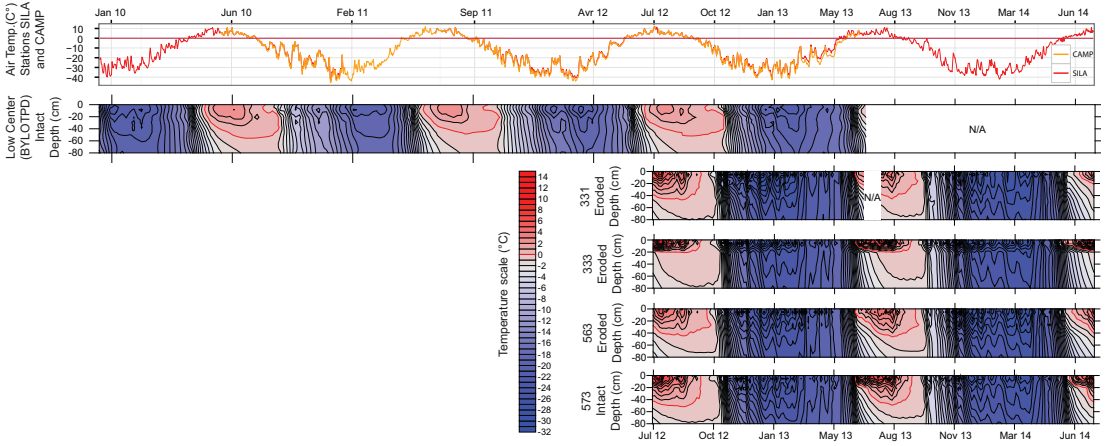

Figure 8. Air Temp (top) represent the mean daily air temperatures from BYLCAMP (yellow) and BYLOSIL (red) recorded between January 2010 to July 2014. The 0 °C limit is highlighted in red as a reference for mean daily air temperature. BYLOTPD, 331, 333, 563 and 573's top 80 cm ground thermal regime follows – dark blue indicate colder temperature, reddish warmer temperature. The 0 °C isotherm of the ground temperature is indicated as a red line.

BGD
12, 11797–11831, 2015